Configurational Thermodynamic Properties of Amorphous Polymers and Polymer Melts. II. Theoretical Considerations

Olagoke Olabisi and Robert Simha*

Department of Macromolecular Science, Case Western Reserve University, Cleveland, Ohio 44106. Received November 18, 1974

ABSTRACT: The three methacrylate polymers and melts of low and high density polyethylenes investigated in the preceding paper are discussed in terms of theory. Corresponding literature data on n-paraffins and hevea rubbers are also considered. The good agreement between experimental and predicted PVT relations obtained for the high polymers is similar to that found earlier in several instances. The extensive results available at present make possible comparisons of the characteristic scaling parameters for different systems, with a variation of the characteristic temperatures by a factor of 2. A relationship between the characteristic compressibility factor or entropy per unit mass and the temperature scaling factor ensues, which results in a correlation between the characteristic segmental energy factor and the two-thirds power of the segmental mass. Proceeding to the pressure dependence of the thermodynamic functions, we find again good agreement between experimental and theoretical energies and entropies. The results once more illustrate the inadequacy of a van der Waals form for the configurational internal energy. The analysis of the liquid–glass transition line in the methacrylate systems yields the variation of the hole fraction $1 - y$ along the boundary for the glasses formed by a variable pressure history, and a satisfactory constancy for the glass formed under atmospheric pressure. From a combination of the theoretical and the experimental equation of state of the latter we derive the temperature and pressure dependence of y and compute an internal energy without further adjustments. Whereas the frozen fraction at T_g, as defined earlier, increases significantly with pressure in polystyrene, it remains nearly constant in the methacrylates. From the magnitude of the hole fractions (or free volumes) it follows that a significant extent of hole clustering should occur in high T_g systems.

In a series of recent papers we have compared experimental results originating from our laboratory or the literature with theoretical predictions. These have included polymers of styrene (PS) and o-methylstyrene (PoMS),[1] atactic and isotactic methyl methacrylate (PMMA),[2,3] vinyl chloride (PVC),[2] and vinyl acetate (PVAC).[4] The results and a detailed examination of dilatometric data at atmospheric pressure[5,6] revealed the good agreement between the experimental and theoretical[5] equations of state.

This enabled us to examine the liquid–glass transition region in terms of the equilibrium theory,[4,7] and to predict the pressure dependence of the glass temperature. Finally we have explored the equation of state of the glass itself and the modifications required in the equilibrium theory and the temperature and pressure dependence of the ordering parameter appearing in the theory.[4,7]

We wish to pursue these directions with the polymers investigated in the preceding paper.[8] The theoretical description of a particular liquid system proceeds in terms of characteristic volume (V^*), temperature (T^*), and pressure (P^*) scaling parameters,[5] which are to reflect structural characteristics of the segment within, of course, the assumptions of the theory. The analysis of the recent liquid state results[8] will enlarge the collection of such parameter values, besides providing the intrinsic information. Considering possible correlations between these quantities,[9] the methacrylates will furnish further examples of relatively high and intermediate T_g systems. The polyethylene melts, on the other hand, represent examples of low T_g's. The scale of T^*'s will be further extended by the inclusion of n-alkanes.[10,11]

Finally we examine the liquid–glass transition zone, the glassy state of the methacrylate polymers, and the comparative behavior of the ordering parameter in the glass.

I. Equation of State

The relations to be employed are in reduced variables[5]

$$\tilde{P}\tilde{V}/\tilde{T} = [1 - 2^{-1/6}y(y\tilde{V})^{-1/3}]^{-1} +$$

$$(2y/\tilde{T})(y\tilde{V})^{-2}[1.011(y\tilde{V})^{-2} - 1.2045] \quad (1)$$

The hole fraction $1 - y$ satisfies the equilibrium condition for an infinite s-mer

$$(s/3c)[1 + y^{-1}\ln(1 - y)] =$$

$$(y/6\tilde{T})(y\tilde{V})^{-2}[2.409 - 3.033(y\tilde{V})^{-2}] +$$

$$[2^{-1/6}y(y\tilde{V})^{-1/3} - \tfrac{1}{3}][1 - 2^{-1/6}y(y\tilde{V})^{-1/3}]^{-1} \quad (2)$$

The (numerical) solution of eq 2 yields y as a function of $\tilde{V}$, $\tilde{T}$, and the "flexibility" ratio $3c/s$, i.e., the number of volume-dependent degrees of freedom per chain segment. For a long chain with a large number of modes of motion this ratio, to be meaningful, must be of the order of unity. The actual value should be a characteristic of the particular system. We have no independent knowledge of this ratio and it cannot be obtained from PVT data without additional assumptions or information, since the appropriate reduced functions, computed for different numerical values, are superimposable.[5] In previous applications we have assigned a universal value of unity to the flexibility parameter. The temperature T^* is defined[5] for a quasilattice of coordination number z by the ratio $(z - 2)s\epsilon^*/(ck)$ and then becomes directly proportional to the intersegmental potential minimum ϵ^*. Moreover, the relation between the effective segment in eq 1 and 2 and the chemical repeat unit will be affected by the requirement $3c/s = 1$. That is, a simple structure such as a polymethylene should require a comparatively larger segmental unit than for example polystyrene.

From the definitions of the scaling parameters (recall that P^* is proportional to the ratio $s\epsilon^*/(sv^*)$, with v^* the segmental hard core volume), combined with the above assumption, we have the relation[2]

$$(P^*V^*/T^*)M_0 = R(c/s) = 27.7 \quad (3)$$

where V^* is expressed in cm^3/g and M_0 is the molecular weight of the segment. Since $sM_0 = (dp)M(\text{monomer})$, dp is the degree of polymerization, there follows

$$c/dp = (P^*V^*/T^*)M(\text{monomer})/R \quad (3')$$

II. Evaluation of Scaling Parameters

A. Atmospheric Pressure. Figure 1 summarizes the volume–temperature results for our three polyethylene melts[8] and Hellwege, *et al.*'s, samples.[12] From the superposition of experimental data on the theoretical line, V^* and T^* are
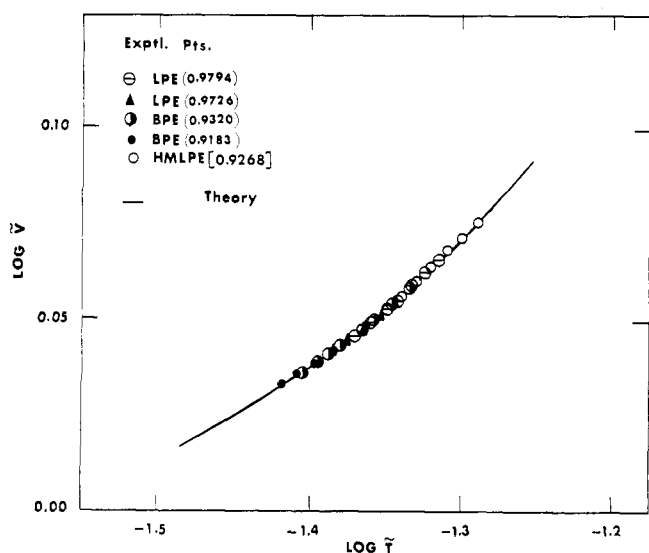
Figure 1. Reduced volume as a function of reduced temperature for polyethylenes at atmospheric pressure.
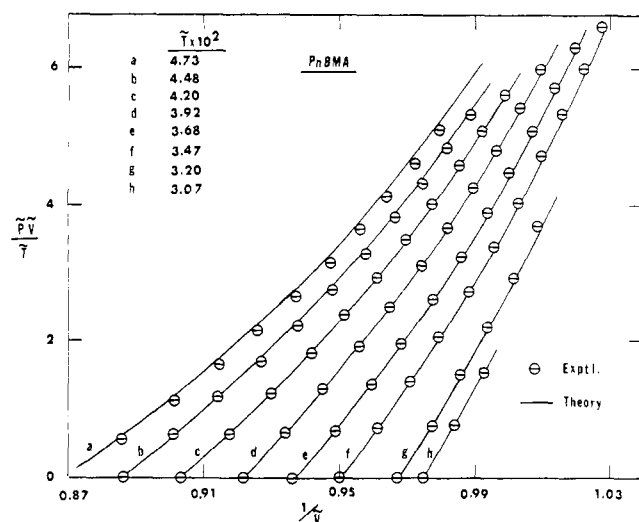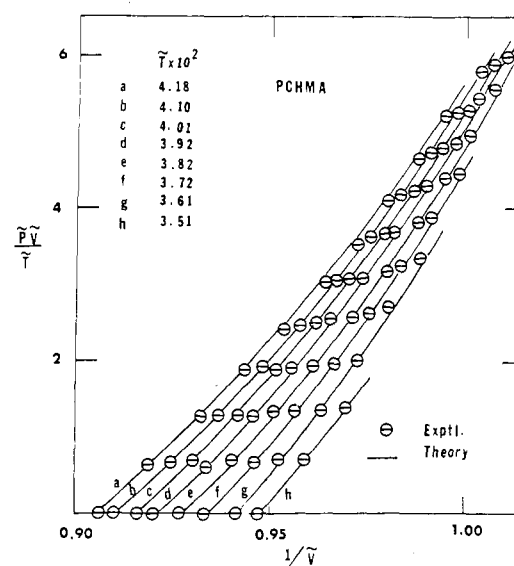

Figure 3. Reduced compressibility factor as a function of reduced density at a series of temperatures for PCHMA.

Figure 2. Reduced compressibility factor as a function of reduced density at a series of temperatures for PnBMA.
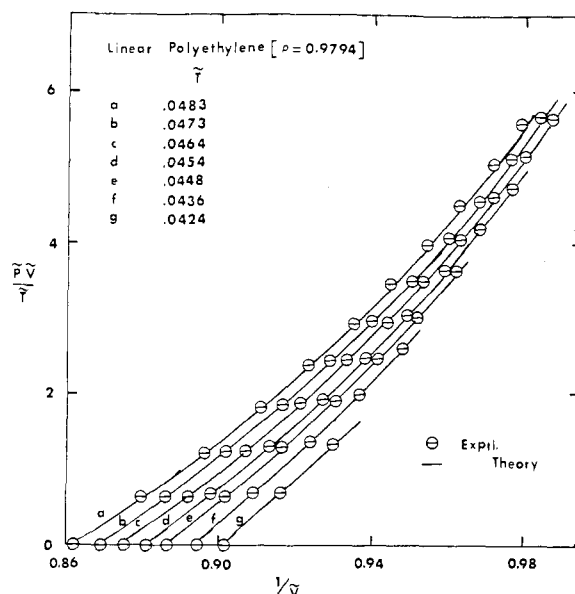

Figure 4. Reduced compressibility factor as a function of reduced density at a series of temperatures for LPE ($\rho = 0.9794$ g/cm^3).

obtained. The agreement noted in Figure 1 is typical of that found earlier for other polymers and oligomers,[2-6] the methacrylates studied in this series,[8] and for hevea rubber and its vulcanizates, as analyzed by Olabisi.[13]

A more severe test of the theory involves an examination of the thermal expansivities.[6] The theoretical isobar in Figure 1 can be accurately represented by a combination of eq 1 when $\tilde{P} = 0$, with eq 2 by means of the interpolation formula[2]

$$\ln (\tilde{V}/0.9018_1) = 23.834_5(\tilde{T})^{3/2} = (\tfrac{2}{3})\tilde{\alpha}\tilde{T}$$

or

$$\tilde{\alpha} = 35.751_8(\tilde{T})^{1/2} \tag{4}$$

in the range $1.65 < \tilde{T} \times 10^2 < 7.03$. Slightly different numerical coefficients over a narrower temperature interval have been derived recently.[4] The differences between experimental and theoretical expansivities are less than 10%.[6] However, eq 4 predicts in general too strong a temperature dependence of α. These departures of the theoretical $\tilde{\alpha}$-$\tilde{T}$ relation can be translated into departures of V^* and T^* from the average value derived by the superposition procedure. Insertion of the experimental α, V, and T values into eq 4 provides a point by point determination of V^* and T^*.

In this manner we observe a maximum increase in T^* and V^* of 5 and 0.3% respectively with increasing T,[13] based on a range of 100°, comparable again with earlier findings.[6]

B. Elevated Pressure. With V^* and T^* determined, P^* is obtained by comparing the theoretical reduced compressibility factor $\tilde{P}\tilde{V}/\tilde{T}$ with the semireduced quantity $P\tilde{V}/\tilde{T}$. The resulting P^* values are averaged over all experimental isotherms. The outcome of this procedure for PnBMA and PCHMA is illustrated in Figures 2 and 3. Due to the low T_g, the widest range of temperatures is available for PnBMA. Deviations from the good agreement between experiment and theory, noticeable otherwise, appear at the highest temperature (199.5°). A similar pattern obtains for PCHMA. The increasing shortening of the pressure range with decreasing temperature is, of course, due to the intervention of the glass transition.

The isotherms for the three polyethylenes are shown in Figures 4-6. The results for Hellwege, *et al.*'s, polymers[12] are very similar.[13] The comparatively small values of T^* result in the highest reduced temperatures for polymers
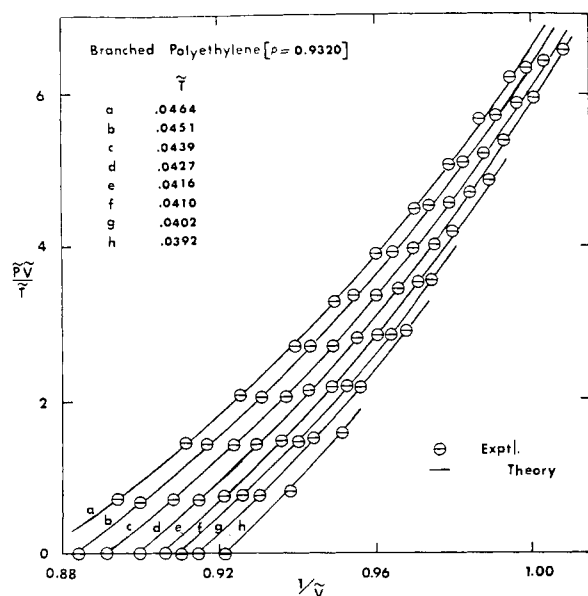
Figure 5. Reduced compressibility factor as a function of reduced density at a series of temperatures for BPE (ρ = 0.9320 g/cm^3).
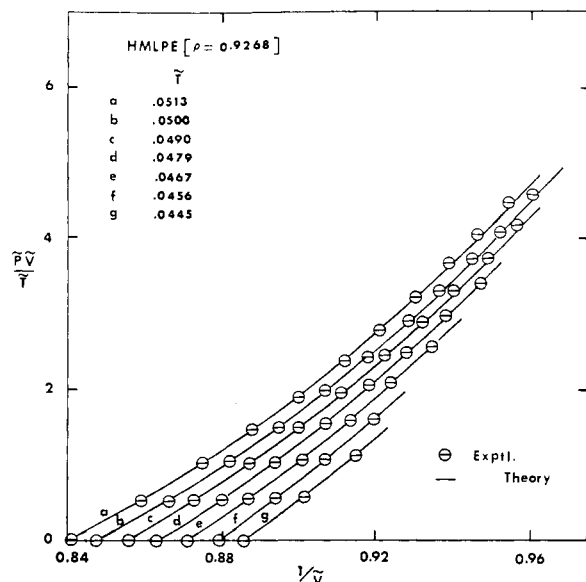

Figure 7. Reduced compressibility factor as a function of reduced density at a series of temperatures for n-tridecane.

Figure 6. Reduced compressibility factor as a function of reduced density at a series of temperatures for HMLPE (ρ = 0.9268 g/cm^3).

Figure 8. Reduced compressibility factor as a function of reduced density at a series of temperatures for n-tetracontane.

studied so far. In the upper temperature and pressure ranges the theoretical compressibility factor tends to be smaller than the experimental one. Since we are dealing with essentially a low-temperature theory, even with the introduction of holes, this trend is consistent.

Figures 7 and 8 describe Doolittle's data on n-alkanes.[10,11] Equations 1 and 2 have been employed without corrections for end effects. This is not sensibly reflected in the results at atmospheric pressure. However, at elevated pressures the agreement between experiment and theory is decidely poorer for the two alkanes, although again better at the lower temperatures. No definite chain-length effect can be extracted from Figures 7 and 8.

Finally, some literature data on hevea rubber[14] have been fitted over a range of $\tilde{T}$ from 2.88 to 3.59 × 10^{-2},[13] with the same degree of success noted in other polymers.

C. The Scaling Parameters. Table I lists T^*, P^*, V^*, and derived quantities for all polymer systems analyzed in this work or previously, in order of increasing T^*. Here E^*
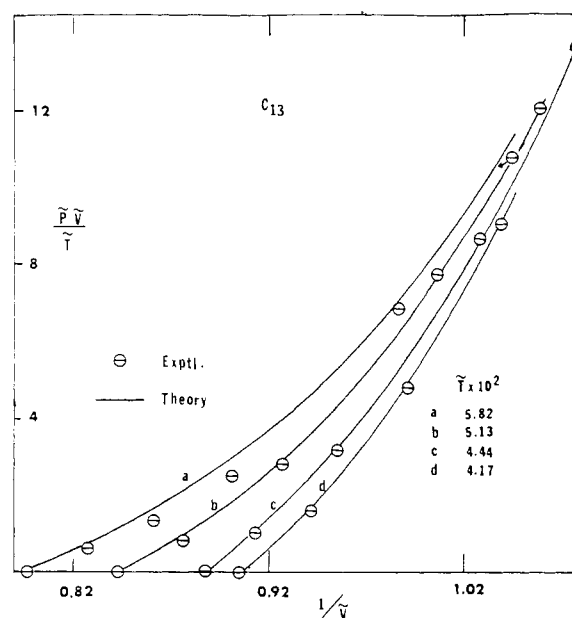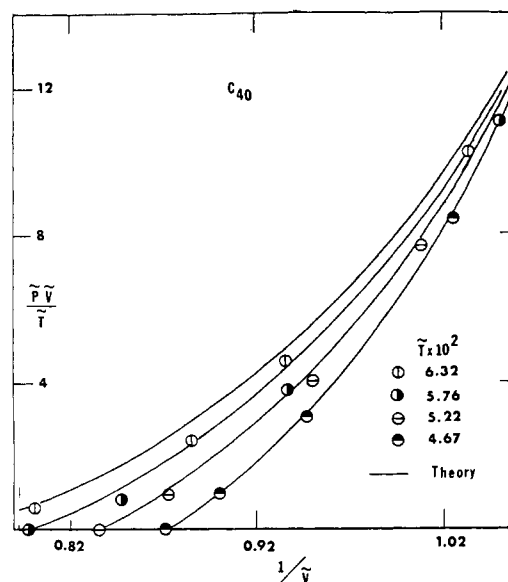
represents the maximum interchain energy $(z - 2)s\epsilon^*$, and the last column equals $kT^*(c/\mathrm{dp})$. For the polyethylenes and n-paraffins the values refer to the methylene unit and thus should be multiplied by two in comparing with other systems. For the high polymers the general trend, starting with polyethylenes, is not unreasonable in the light of expected intersegmental energies. However, the expected trend in respect to T^* is interrupted at several places. For example, PVAC (No. 10) seems too low. The difference between the NBS polyethylenes (No. 11 and 17) is small, actually of the same order as that observed in ref 12 (No. 16 vs. 18), although the T^*'s are larger. An enhancement of the segmental attraction in the branched species is reasonable. The reason for the lower T^* of HMLPE (No. 9) compared with LPE is not obvious. An increase of T^* in hevea with increasing sulfur content (No. 12–14) would not be inconsistent, considering our treatment of a molecule with two different repeat units as a homogeneous chain. However, the differences are too small to be significant. The

Table I
Characteristic Parameters and Related Quantities

|	Material	T^*, °K	V^*, cm³/g	P^*, bar	T_g, °K	P^*V^*/T^* (bar cm³)/(g °K)	M_0	M_0/M_{repeat}	M_0V^*	c/dp	E^*/dp, cal × 10⁻²³
1	C_7	5888	1.2365	7648		1.6061	17.2	1.20	21.3	0.55	536
2	C_9	6500	1.2235	7600		1.4306	19.4	1.36	23.7	0.49	525
3	C_{11}	6910	1.2131	7580		1.3310	20.8	1.47	25.2	0.45	518
4	C_{13}	7277	1.2059	7552		1.2515	22.1	1.56	26.7	0.43	512
5	C_{17}	7797	1.1955	7520		1.1530	24.0	1.70	28.7	0.39	504
6	C_{20}	7979	1.1900	7490		1.1171	24.8	1.76	29.5	0.38	499
7	C_{30}	8700	1.1800	7460		1.0118	27.4	1.95	32.3	0.34	491
8	C_{40}	9068	1.1738	7433		0.9622	28.8	2.05	33.8	0.33	486
9	HMLPE	9205	1.1285	8968	(191)	1.0994	25.2	1.80	28.4	0.37	562
10	PVAc	9412	0.8140	9408	304	0.8137	34.0	0.79	27.7	0.84	2612
11	LPE	9772	1.1417	7478	(203)	0.8737	31.7	2.26	36.2	0.29	474
12	H. Rubber	9831	1.0774	7465	204	0.8181	33.9	1.00	36.5	0.67	2169
13	HR–6% S	9877	1.0286	8690	226	0.9050	30.6				
14	HR–11.5% S	9925	0.9743	10269	252	1.0080	27.5				
15	PnBMA	9988	0.9299	8456	293	0.7873	35.2	0.50	32.7	1.34	4429
16	LPE[12]	10046	1.1548	7160	(208)	0.8231	33.7	2.41	38.9	0.28	459
17	BPE	10139	1.1601	6946	(210)	0.7948	34.9				
18	BPE[12]	10328	1.1641	6765	(214)	0.7625	36.3				
19	i-PMMA	11170	0.8160	10088	320	0.7370	37.6	0.75	30.7	0.89	3266
20	PCHMA	11290	0.8906	8382	380	0.6612	41.9	0.50	37.3	1.34	4975
21	PVC[12]	11320	0.7105	10345	349	0.6493	42.7	1.38	30.3	0.48	1808
22	PMMA[12]	11890	0.8350	9303	378	0.6533	42.4	0.84	35.4	0.79	3081
23	PMMA	11920	0.8370	9147	378	0.6423	43.1	0.86	36.1	0.77	3037
24	PS	12680	0.9598	7453	365	0.5641	49.1	0.94	47.1	0.71	2951
25	PS[12]	12700	0.9625	7638	362	0.5789	48.0	0.92	46.2	0.72	3033
26	PoMS	12740	0.9762	7458	404	0.5715	48.5	0.82	47.3	0.82	3437
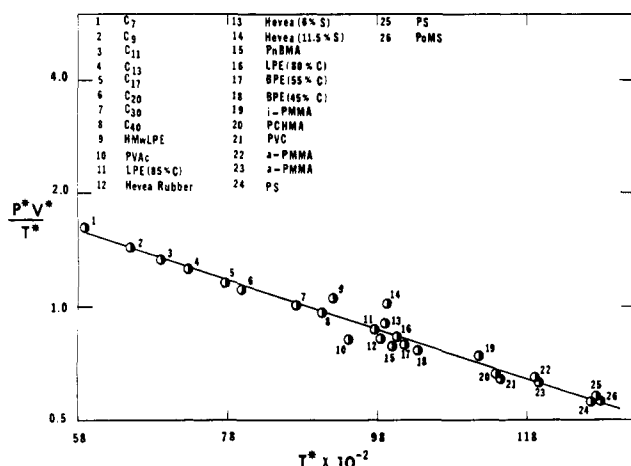
Figure 9. Correlation between characteristic compressibility factor and characteristic temperature for polymers and oligomers appearing in Table I. Solid line, eq 5.

trend in T^* and T_g has been discussed previously. Their ratio varies from about 0.036 for high T_g polymers to 0.026 for a SBR rubber.[6] For the three heveas this ratio changes from 0.021 to 0.025. Assuming the smaller value for the ethylenes, the T_g's indicated in parentheses are obtained. They happen to be in the range advocated in the literature by one group of investigators. Both the vulcanized rubbers and HMLPE have comparatively large P^* or characteristic energy densities, a possible reflection of an enhanced entanglement density.

We note next the relationship between M_0 and M_{repeat}, the average molecular weight per backbone carbon atom. For the two highly structured methacrylate polymers (No.

15 and 20), the ratio assumes a minimum value of 0.50, with larger numbers for the PMMA's (No. 19, 22, 23), the styrenes (No. 24–26), and PVAC. A still larger value ensues for PVC (No. 21). Finally, for the linear polyethylenes, M_0 corresponds to about two methylene units.

The molar segmental volumes M_0V^* should represent a compromise between the size and structure of the monomer unit. For example, the magnitudes for LPE and PMMA are practically identical because the condition $3c/s = 1$ can be satisfied in a smaller unit in PMMA than in the simple structure of ethylene units. The considerable differences between PS and PCHMA point to a similar effect. The values of the ratio c/dp again reflect the structural influence between the two extremes of the polyethylenes vs. PnBMA and PCHMA. The reasons for the difference between HMLPE and LPE in respect to segmental characteristics, see M_0V^* and c/dp, are not clear. The difference between the stereoregular and conventional PMMA is of interest and in accord with the enhanced flexibility suggested as a reason for the lower T_g of the former.[15]

Finally, we consider the maximum attractive energies per monomer unit, E^*/dp. Again, the limits are represented by the polyethylenes and methacrylates (No. 15 and 20). The value for PVC seems comparatively low and that for natural rubber high.

The data collected in Table I permit the exploration of a correlation between the scaling parameters suggested earlier.[9] Figure 9 shows a plot of the reducing compressibility or entropy scaling factor per unit mass vs. T^* on a semilogarithmic scale. A single line can be constructed which encompasses both oligomers and polymers with some scatter. This correlation makes possible the estimation of P^* and hence of high-pressure densities by means of atmospheric pressure data. The equation of the line is
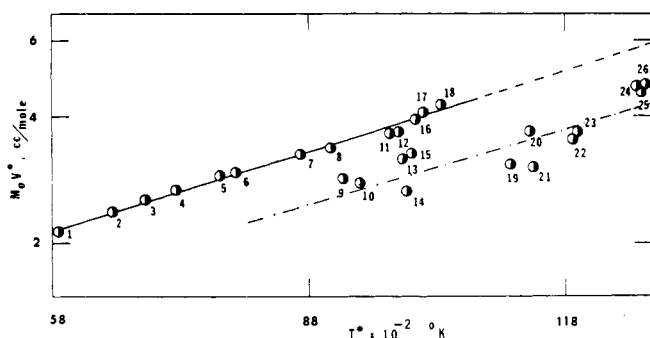
Figure 10. Correlation between characteristic segmental volume M_0V^* and characteristic temperature for polymers and oligomers appearing in Table I. Solid lines, eq 6a and 6b.

$$\ln (P^*V^*/T^*) = 1.319_1 - (3/2.01)(T^* \times 10^{-4})$$

or

$$10^{-4}T^* = \ln (M_0/7.406_7)^{2 \cdot 01/3} \tag{5}$$

In other words, the characteristic segmental energy ϵ^* is related to the $\frac{2}{3}$ power of the segmental mass. The most pronounced positive deviations from the linear correlation in Figure 9 occur for HMLPE and the vulcanized rubbers. Since P^* and T^* are usually the quantities most subject to variations, this implies larger than "normal" values for either or both. This is not inconsistent with an enhanced characteristic energy parameter due to cross-linking, which in our treatment is effectively an average over two types of chain units. The observed difference between the three hevea polymers would tend to support this. A similar argument for HMLPE is invalidated by the small T^* in comparison with the other polyethylenes. The reasons for the negative deviation in PVAc are not obvious. We note only a similar, but less pronounced, tendency in PnBMA. The departures, at any rate, are too large to be caused by experimental error solely.

The appearance of the $\frac{2}{3}$ power in eq 5 suggests a relation involving the segmental surface. In Figure 10 the molar volume M_0V^* is plotted as a function of T^*. No single correlation line for all systems examined in Figure 9 results. The hydrocarbons, including the hevea rubber, can with fair accuracy be represented by the equation

$$10^{-4}T^* = \ln (M_0V^*/9.3)^{2 \cdot 1/3} \tag{6a}$$

whereas the remaining systems scatter around a line, the equation of which is

$$10^{-4}T^* = \ln (M_0V^*/7.4)^{2 \cdot 2/3} \tag{6b}$$

nearly parallel to the other.

To conclude this section, we examine the dependence of the scaling parameters on chain length for the n-alkanes. On multiplying the specific volumes V^* in Table I by the factor $14n + 2$, we obtain with a maximum deviation of 0.2% the expression

$$V^*(cm^3/mol) = 43.31 + 16.23(n - 2) \tag{7}$$

$$9 \leq n \leq 40$$

That is, the ratio V_m^*/V_e^* between the middle and terminal segments equals $16.23/21.65 = 0.75$. This may be compared with an earlier determination by Simha and Havlik.[16] The transformation relations from their reduced coordinate system to the present one are

$$\tilde{V}_H = \tilde{V} \times 1.0347; \quad \tilde{T}_H = \tilde{T}/0.5122 \tag{8}$$

In this manner one finds $V_m^*/V_e^* = 16.30/23.31 = 0.70$. Hijmans[17] obtains by application of the corresponding
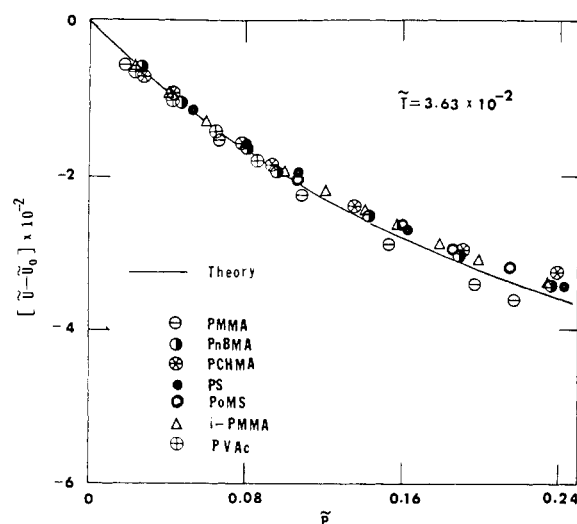

Figure 11. Change of reduced configurational internal energy as a function of reduced pressure at constant temperature for several polymers.

state principle $V_m^*/V_e^* = 0.71$. Next we derive the expression

$$c = 1.232 + 0.14(n - 2) \tag{9a}$$

or $c_m/c_e = 0.23$. Previous values[16,17] for c_m are about 0.16. The temperature and pressure parameters can be fitted to the following expressions

$$T^* = 9475(1 - 2.81/n); \quad P^* = 7403(1 + 0.244/n)$$

$$7 \leq n \leq 40 \tag{9b}$$

with maximum errors of 3 and 0.2%, respectively. The limiting values are close to those for our LPE, see Table I and Figure 9.

III. Thermodynamic Functions

Here we consider the configurational contributions to the internal energy $\tilde{U}$ and entropy $\tilde{S}$. The expression for the former is

$$-2\tilde{U} = y(y\tilde{V})^{-2}[2.409 - 1.011(y\tilde{V})^{-2}] \tag{10}$$

From the standard formula

$$S/k = \ln Z_{conf} + T(\partial \ln Z_{conf}/\partial T)_V$$

and the expression for the configurational partition function Z_{conf} we derive

$$S/(Nkc) - \ln V^* = -\ln y/c -$$

$$(s/c)(1 - y) \ln (1 - y)/y + 3 \ln [y\tilde{V}^{1/3} - 2^{-1/6}y] \tag{11}$$

where the reduction factor for S may be written as P^*V^*/T^*. Clearly the first term on the right-hand side is negligible here. Having determined earlier y as a function of $\tilde{V}$ and $\tilde{T}$ by means of eq 2, we can now compute the difference

$$\Delta\tilde{Q} = \tilde{Q}(\tilde{V}, \tilde{T}) - \tilde{Q}(\tilde{V}_0, \tilde{T})$$

where $\tilde{Q} = \tilde{U}$ or $\tilde{S}$ and the subscript refers to atmospheric pressure. The experimental quantities are obtained from the Tait equation. The expression for ΔU has been given previously,[1] and from the relation

$$TdS = dU + PdV$$

there follows

$$T\Delta S = \Delta U + B(V_0 - V) - CV_0P \tag{12}$$

As an example a reduced isotherm is displayed in Figure 11. Results for the two styrene systems and the two PMMA's at similar temperatures have been shown pre-
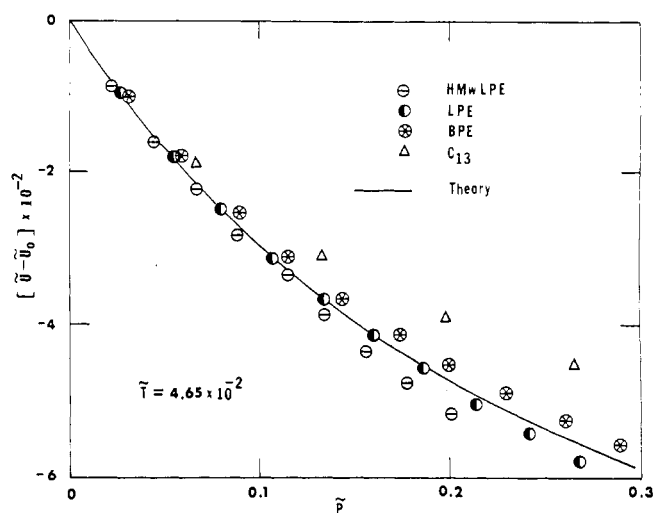
Figure 12. Change of reduced configurational internal energy as a function of reduced pressure at constant temperature for polyethylenes and n-C_{13}.
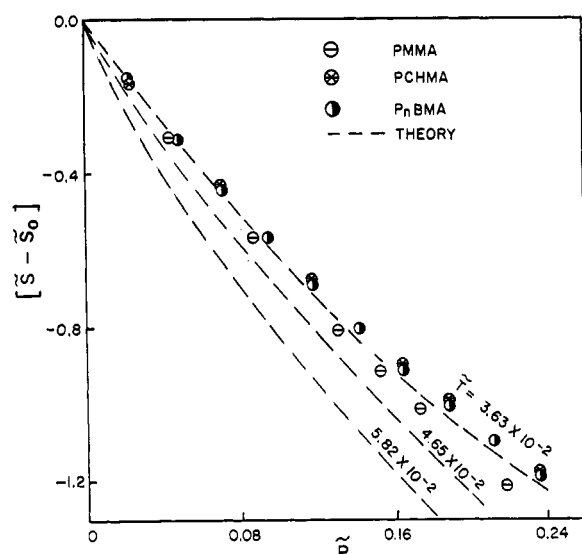

Figure 14. Reduced internal pressure $\tilde{P}_i$ as a function of reduced volume at constant temperature.

Figure 13. Change of reduced configurational entropy as a function of reduced pressure at several temperatures.

Figure 15. Variation of hole fraction $Z = 1 - y$ with pressure along liquid–glass transition line for LPG and HPG of methacrylates. For explanation see text.

viously.[1,3] They are combined here with the data derived from the recent measurements,[8] in order to illustrate the aggregate agreement between theory and experiment and thus the validity of a corresponding states principle. No disposable parameter remains of course in this construction. Larger departures for the oligomer are seen in Figure 12, which also contains the polyethylenes. We note in Figure 13 the corresponding agreement in respect to the entropy changes, which is to be expected in view of the results shown in Figures 2–6.

The theoretical internal pressures P_i are known to exhibit larger deviations.[1,3,4] Since $P_i = (\partial U/\partial V)_T$, this is anticipated from the appearance of Figure 11. The results for the polymers shown in this graph appear in Figure 14. They also serve to illustrate again the inadequacy of a van der Waals expression for the internal energy.

IV. Glassy State Relationships

A. Liquid–Glass Transition. Within the frame of the theory by now extensively employed in the analysis of the liquid state, it is natural to examine the behavior of the ordering parameter y along the transition line, *i.e.*, the inter-
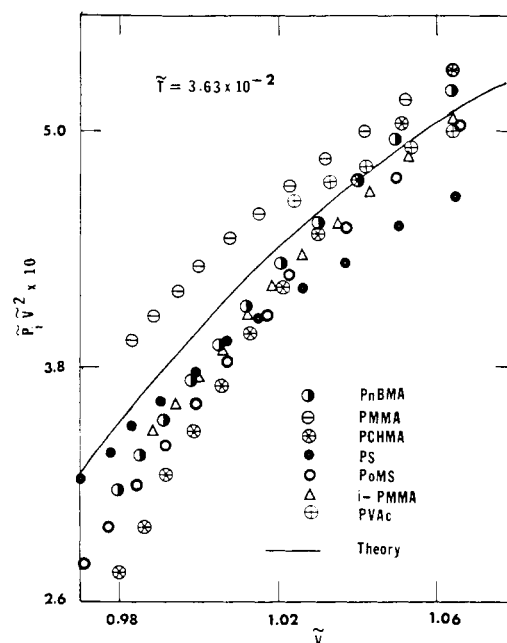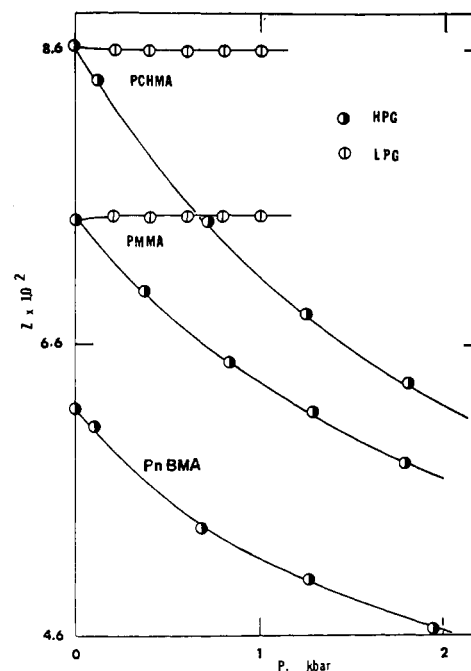
section between the liquid and glassy surfaces in PVT space.[4,7] The latter has been formed in our experiments by pressurizing the melt to different extents and subsequently cooling,[1,7,8] and thus the formation histories of these "high pressure glasses" (HPG) are variable. A particular constant formation glass corresponding to cooling under atmospheric pressure (LPG) has been defined quantitatively by an extrapolation of isothermal data[1,9] rather than by isobaric experimentation. For LPG therefore, the transition should be characterized by a single value of y, whereas for HPG y is expected to increase with pressure. Figure 15 illustrates the behavior of the hole fraction $Z = 1 - y$ for the three methacrylates, as computed from the observed transition

temperatures and pressures with the aid of eq 1 and 2. The low T_g of PnBMA prevents an adequate characterization of its LPG. Z is observed to remain satisfactorily constant in LPG in contrast to the significant decrease for HPG.

Similar results have been obtained for PS and PoMS,[7] and more recently for poly(vinyl acetate),[4] based on directed isobaric measurement. One may proceed further in testing the theory by comparing the pressure coefficients of the glass temperatures of HPG and LPG by means of the equation

$$dT_g/dP = (\partial T_g/\partial P)_Z + (\partial T_g/\partial Z)_P \, dZ/dP \quad (13)$$

The first derivative on the right-hand side equals the ratio $\Delta\kappa/\Delta\alpha$,[7,18] the third is obtained experimentally, see Figure 15, whereas the second is derived from eq 1 and 2.

The quantitative prediction of the left-hand side for the two styrene polymers[7] turns out to be comparable or superior to that offered by other authors on more intuitive grounds; however, significant positive deviations remain up to a pressure of about 1600 bar. In the case of PVAc, two constant formation glasses were obtained experimentally.[18] A gratifying agreement with eq 3 indeed ensues. For PCHMA and PMMA it is less satisfactory and of about the same extent as in the two styrenes. For PMMA, dT_g/dP equals $2.3_6 \times 10^{-2}$ bar^{-1} whereas the computed values vary from 2.57 to 1.41 between 1 and 1270 bar. The corresponding numbers for PCHMA are $2.2_4 \times 10^{-2}$ vs. a variation from 3.14 to 2.47 in about the same range of pressures. Thus both positive and negative departures from eq 10 occur, which may well reflect inaccuracies in the determination of derivatives, arising from the extrapolation in obtaining the LPG data.

B. Equation of State for LPG. The ad hoc assumption is frequently adopted not only in thermodynamic treatments but also in approaches based on specific models, that the glassy state can be characterized by the constancy of structural parameters. In the liquid state, the dependence of these parameters on the variables of state is uniquely determined by the minimization of an appropriate configurational free energy. The quantity to consider here then is y in conjunction with the equation of state

$$-P = (\partial F/\partial V)_T = (\partial F/\partial V)_{T,y} +$$

$$(\partial F/\partial y)_{V,T}(\partial y/\partial V)_T \quad (14)$$

The last term vanishes at equilibrium, due to the condition expressed by eq 2, and it also disappears for constant y. But it has been demonstrated extensively at atmospheric and elevated pressures that a constant hole fraction $Z = 1 - y$ is in definite disagreement with experiment.[3,4,6,7,19] This, we stress, is in contrast to the good agreement between the experimental and theoretical equations of state under conditions of thermodynamic equilibrium, when Z is determined as the solution of eq 2. For example, the computed thermal expansivities are significantly smaller than is observed. In other words, a significant contribution to the configurational properties arises from the temperature and pressure variation of the hole fraction and remains well below T_g. This contribution practically vanishes only in the range of 50–70°K, as we have demonstrated for a variety of organic polymers by comparing experimental and theoretical thermal expansivities.[20]

Our procedure so far has been to treat y as a disposable parameter in eq 1, to be derived from PVT data. As an illustration, results for PMMA at two pressures appear in Figure 16, where also the isobaric dependence of $1 - y$ on temperature, eq 2, is extrapolated into the glassy domain. The changes in slope caused by the glass transition as well as by a β relaxation are clearly seen. The pressure indepen-
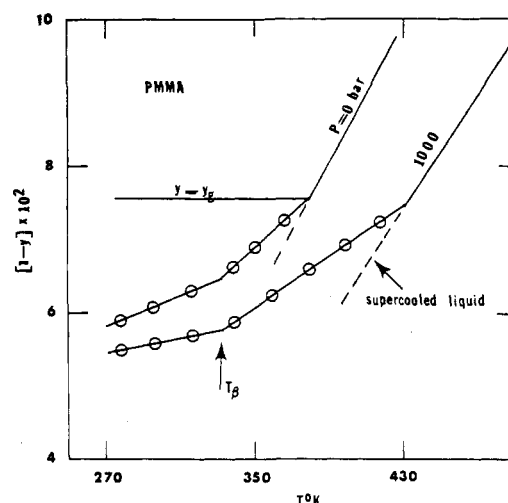

Figure 16. Variation of hole fraction $1 - y$ with temperature in liquid and glassy state above and below β-relaxation region of PMMA at two pressures.
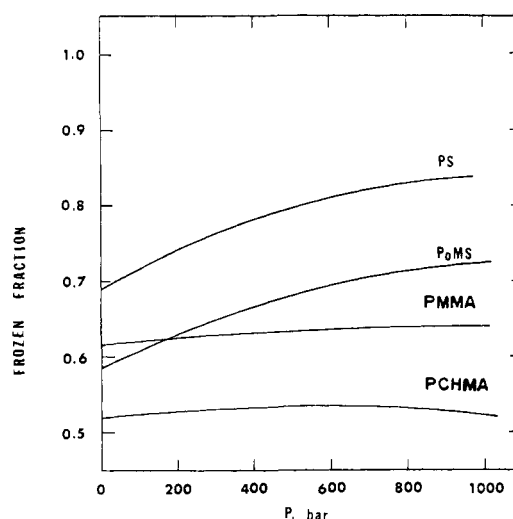

Figure 17. Variation of frozen fraction at T_g, eq 15, with pressure.

dent location of the latter is consistent with observations by Heydemann and Guicking,[21] and more recent results by Quach, et al.[3] An explicit equation of state results from a combination of eq 1 with an empirical expression for y as derived for example from Figure 16, and the experimental pressure dependence of T_g for LPG.[7] For detailed results on the methacrylates ref 13 should be consulted.

A numerical measure of extent of freeze-in is provided by the ratio f_T[6]

$$f_T = 1 - (\partial Z/\partial T)_P/(\partial Z/\partial T)_{P,l} \quad (15)$$

where the first derivative refers to LPG and the second to the liquid, both at $T = T_g$. We have previously shown that at atmospheric pressure f_T tends to increase for different polymers with decreasing (reduced) glass temperature.[6] The pressure dependence of f_T for four polymers is exhibited in Figure 17. A pronounced increase or reduction of the liquid-like character with increasing pressure in the glassy styrene polymers is to be contrasted with a near constancy in the methacrylates. Here both temperature coefficients in eq 15 are affected by pressure to nearly the same degree. It may be noted that the two styrenes have nearly identical pressure coefficients $dT_g/dP \simeq 0.073$, as do the methacrylates but with smaller values, viz., $\simeq 0.06$–0.05. Note that these values, of course, refer to LPG and there-
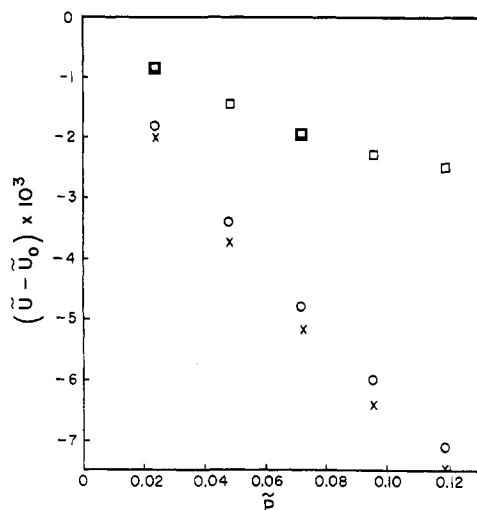
Figure 18. Compressional energy change of PCHMA (LPG), $T =$ 353°K: crosses, experimental (Tait equation); circles, eq 10, hole fraction derived from equation of state; squares, constant hole fraction.

fore exceed those quoted in connection with eq 13. One may surmise that these differences between the two sets of polymers are related to the differences in the character of the side chains.

We have derived the variation of the ordering parameter by simply combining the equation of state (eq 1) with experimental data. This procedure is not consistent with eq 14, although it does not, of course, affect the important conclusion that y is not constant. In other words, the equation of state is not derived from a partition function, characteristic of a particular thermal theory history of the glass in question. An analogous inconsistency is inherent in a computation of the internal energy from eq 10. Alternatively we may regard this relation as the summation of a lattice energy, with y determined empirically from the equation of state. The experimental energy change on compression can again be obtained from the Tait equation, as for the liquid,[1] see Figures 11 and 12. An example is shown in Figure 18 which displays three computations of an isotherm for PCHMA. A close agreement between the experimental and "variable y" results is noted, whereas the "frozen y" energy is completely off. A quantitatively similar relationship is observed in PVAc.[22] Analogous large and smaller deviations respectively result in respect to the internal pressure.[23]

We conclude with a comment on the size distribution of inhomogeneities described in the present treatment as holes. Size distributions of holes have been considered by several authors in connection with equilibrium and particularly transport processes. In the frame of a lattice model, this implies a consideration of hole clusters, where by assumption a singlet hole is equivalent to a chain segment of the size shown in Table I.

The hole fractions at the glass temperatures and atmospheric pressure for most of the polymers listed in Table I and other systems have been shown to vary between about 10% for poly(α-methylstyrene) and 1% for poly(dimethylsiloxane) and an SBR rubber.[6] Assuming for the sake of consistency with the numerical assignments in eq 1 a coordination number of 12 in the quasi-lattice, the computed number average cluster size varies between 2.5 and 1.06. The corresponding singlet to doublet number ratios are 4.8:1 and 18:1, with, of course, an appreciable number of higher multiplets present in the high T_g polymers. Such clusters can be expected to impart "liquid-like" character-

istics to the glass. We note that for the styrene polymer, the ratio $1 - f_T$ equals 0.54. For PMMA and PCHMA $1 - y_g$ is about 7.3 and 8.5%, with $1 - f_T$ equal to 0.37 and 0.48, respectively.

V. Conclusions

The equation of state and derived thermodynamic functions have been examined for a broad range of amorphous polymers in terms of the hole theory. The characteristic scaling parameters, in particular the temperature, cover a correspondingly wide range of numerical values. The quantitative success of the theory gives us confidence in computing configurational thermodynamic quantities which are not readily accessible to experimental determination.

In regard to the liquid–glass intersection, the theoretical prediction of the differences between the pressure coefficients dT_g/dP of HPG and LPG is here only semiquantitative. However, more direct experimentation[4] than we have undertaken indicates a more satisfactory agreement between experiment and theory in the case of poly(vinyl acetate). We show once more that the postulate of completely frozen configurational contributions in the glass is inappropriate at elevated temperatures, where a significant liquid-like contribution remains, contrary to views expressed in the literature. It is only gradually eliminated with decreasing temperature and, at a lesser rate, with increasing pressure. While the quantitative results are, of course, tied to the specific theoretical formulation, this behavior should be regarded as a general characteristic of the glassy state. This is also supported by the results of low-temperature dilatometric experiments. In the present state of theory, we characterize these gradual changes in terms of the hole $(1 - y)$ or the frozen (f_T) fraction. These quantities are treated as disposable parameters in the equation of state originally derived for the equilibrium liquid. It is noteworthy that this yields a quite satisfactory result for the compressional energy change of the glass without further adjustable parameters.

A more consistent procedure also yields more accurate predictions of the thermodynamic functions. These are derived from a partition function which includes the dependence of y on the variables of state as obtained from experiment by means of the *complete* eq 14.[22]

References and Notes

(1) A. Quach and R. Simha, *J. Appl. Phys.*, **42**, 4592 (1971).
(2) R. Simha, P. S. Wilson, and O. Olabisi, *Kolloid-Z. Z. Polym.*, **251**, 402 (1973).
(3) A. Quach, P. S. Wilson, and R. Simha, *J. Macromol. Sci., Phys.*, **9**, 533 (1974).
(4) J. E. McKinney and R. Simha, *Macromolecules*, **7**, 894 (1974).
(5) R. Simha and T. Somcynsky, *Macromolecules*, **2**, 342 (1969).
(6) R. Simha and P. S. Wilson, *Macromolecules*, **6**, 908 (1973).
(7) A. Quach and R. Simha, *J. Phys. Chem.*, **76**, 416 (1972).
(8) O. Olabisi and R. Simha, preceding paper in this issue.
(9) A. Quach, Ph.D. Thesis, Case Western Reserve University, 1971.
(10) A. K. Doolittle and D. B. Doolittle, *AIChE J.*, **6**, 150 (1960).
(11) A. K. Doolittle, *J. Chem. Eng. Data*, **9**, 275 (1964).
(12) K. H. Hellwege, W. Knappe, and P. Lehmann, *Kolloid-Z. Z. Polym.*, **183**, 110 (1962).
(13) O. Olabisi, Ph.D. Thesis, Case Western Reserve University, 1973.
(14) A. H. Scott, *J. Res. Nat. Bur. Stand.*, **14**, 99 (1935).
(15) F. E. Karasz and W. J. MacKnight, *Macromolecules*, **1**, 537 (1968).
(16) R. Simha and A. J. Havlik, *J. Amer. Chem. Soc.*, **86**, 197 (1964).
(17) J. Hijmans, *Physica (Utrecht)*, **27**, 433 (1961).
(18) J. E. McKinney and M. Goldstein, *J. Res. Nat. Bur. Stand., Sect. A*, **78**, 331 (1974).
(19) T. Somcynsky and R. Simha, *J. Appl. Phys.*, **42**, 4545 (1971).
(20) R. Simha, J. M. Roe, and V. S. Nanda, *J. Appl. Phys.*, **43**, 4312 (1972).
(21) P. Heydemann and H. D. Guicking, *Kolloid-Z. Z. Polym.*, **193**, 16 (1963).
(22) J. E. McKinney and R. Simha, in preparation for publication.
(23) O. Olabisi, unpublished.